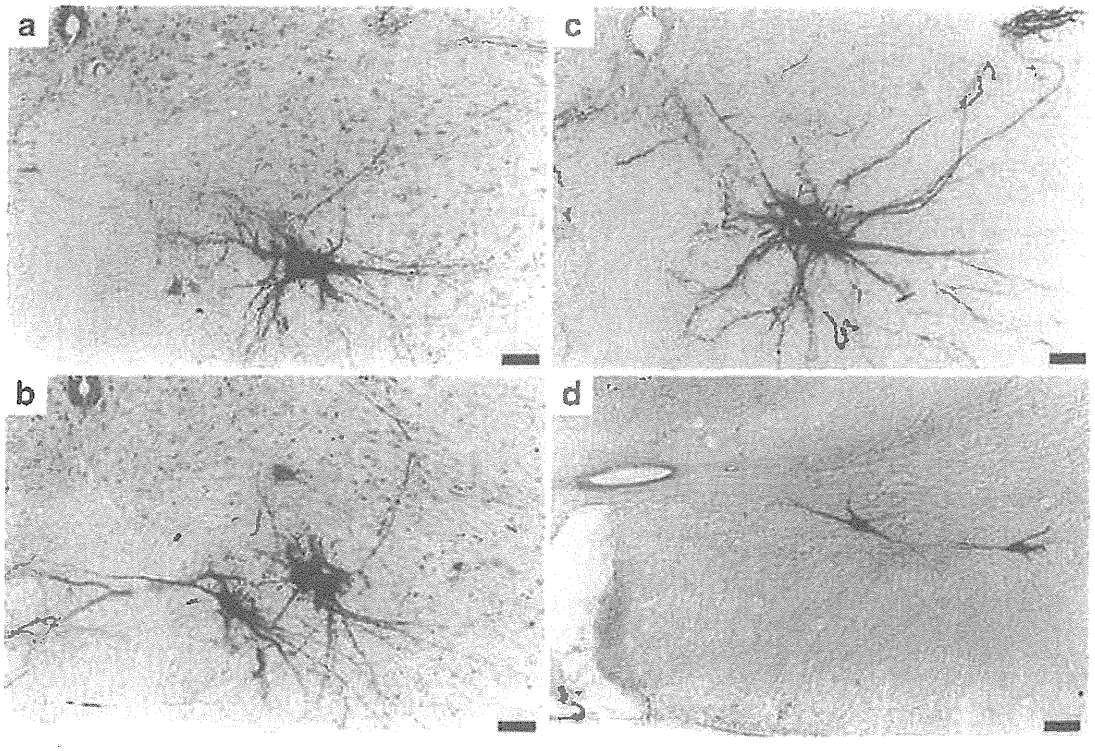

Fig. 9.1 Photomicrographs showing wheat germ agglutinin-horseradish peroxidase-labeled spinal accessory motoneurons. (**a**) A motoneuron at C2–C3 segments in a representative control ICR mouse; (**b**) site A in the *twy* mouse, the most rostral level; (**c**) site B, the level immediately rostral to the compressive lesion; (**d**) site C, the site of mechanical compression at C2–C3 cord segments. The *top side* in each panel represents the dorsal aspect of the cord. Scale bar = 50 μm (Reprinted, with permission, from [7])

9.1.3 Localization of Brain-Derived Neurotropic Factor Immunoreactivity in the Anterior Gray Matter and Its Relationship to the Magnitude of Compression

At site B, BDNF immunoreactivity in the anterior horn cells of *twy* mice was significantly higher than in ICR and site A in *twy* mice (Fig. 9.3c). More severe compression at site C (TRAS < 50 %; $n = 8$) correlated with increased BDNF immunoreactivity in anterior horn cells at site B. Also, more labeled non-neuronal astroglia- and microglia-like cells were detected at sites B and C.

9.1.4 Localization of Neurotrophin-3 Immunoreactivity in the Anterior Gray Horn and Its Relationship to the Magnitude of Compression

At site B in *twy* mice, immunostaining for NT-3 V4 antibody was significant in the anterior horn cells, with enhanced immunoreactivity in the neuron soma and dendrites (Fig. 9.4c) compared with those seen at site A in *twy* and ICR mice.

Table 9.1 Results of morphological measurements of neuronal soma and dendrites of the wheat germ agglutinin-horseradish peroxidase-labeled spinal accessory motoneurons in the medial cell pool of the *twy* and control ICR mice

	Spinal cord level				
	Site A[a]	Site B[b]	Site C[c]	Mean (SD)	Total number (SD)
twy mouse ($n=30$)					
1. Neuron					
Number	34.7 (10.1)	67.9 (10.5)*	3.7 (3.2)**		106.3 (18.1)*
Area of soma (μm2)	574.0 (138.4)*	565.9 (98.9)*	324.4 (170.7)	488.0 (180.2)**	
Number of segments	7.4 (1.1)	7.6 (1.0)	5.7 (1.1)	6.9 (1.4)	
Maximum branch order	3.0 (0.8)	3.1 (0.7)	2.8 (0.7)	3.0 (0.7)	
Total length (μm)	577.0 (142.5)*	523.8 (157.8)*	242.6 (150.8)	242.6 (150.8)	
Maximum branch length (μm)	190.6 (61.5)	183.1 (61.1)	96.9 (50.1)	156.9 (71.4)*	
ICR mouse ($n=6$)					
1. Neuron					
Number	29.5 (12.1)	93.7 (10.0)	24.3 (5.5)		145.8 (17.0)
Area of soma (μm2)	529.2 (44.1)	519.4 (46.9)	526.3 (83.8)	524.8 (57.5)	
2. Dendrite					
Number of segments	7.5 (1.0)	8.3 (0.5)	6.2 (1.2)	7.3 (1.3)	
Maximum branch order	3.2 (0.8)	3.2 (0.8)	3.0 (0.9)	3.1 (0.8)	
Total length (μm)	531.8 (79.2)	418.3 (1.3)	435.6 (169.4)	461.9 (134.0)	
Maximum branch length (μm)	169.3 (28.7)	123.0 (40.7)	118.6 (38.2)	137.0 (41.4)	

*$P<0.05$, **$P<0.01$ (Wilcoxon's signed-ranks test), compared with the corresponding data of ICR mice

[a]Site A: the level most rostral to C1 ventral root. Values are mean (SD)

[b]Site B: the level immediately rostral to the compression lesion between C1 ventral and C2 dorsal roots

[c]Site C: compression site between C2 and C3 dorsal roots (Reprinted, with permission, from [7])

9.1.5 *Topographic and Quantitative Analysis of Brain-Derived Neurotropic Factor and Neurotrophin-3 Immunoreactivity*

BDNF was detected as a band with a molecular weight of 17–19 kDa (Fig. 9.5a) and NT-3 as a 30 kDa band (Fig. 9.5b). At site B in *twy* mice, BDNF and NT-3 expression was 70.7 % (*lane 6* in Fig. 9.5a) and 72.7 % (*lane 6* in Fig. 9.5b), respectively ($P<0.05$) when compared with that at site C. Immunoreactivity of both neurotrophins increased significantly at the level distal to the compressed segment (*lane 8*).

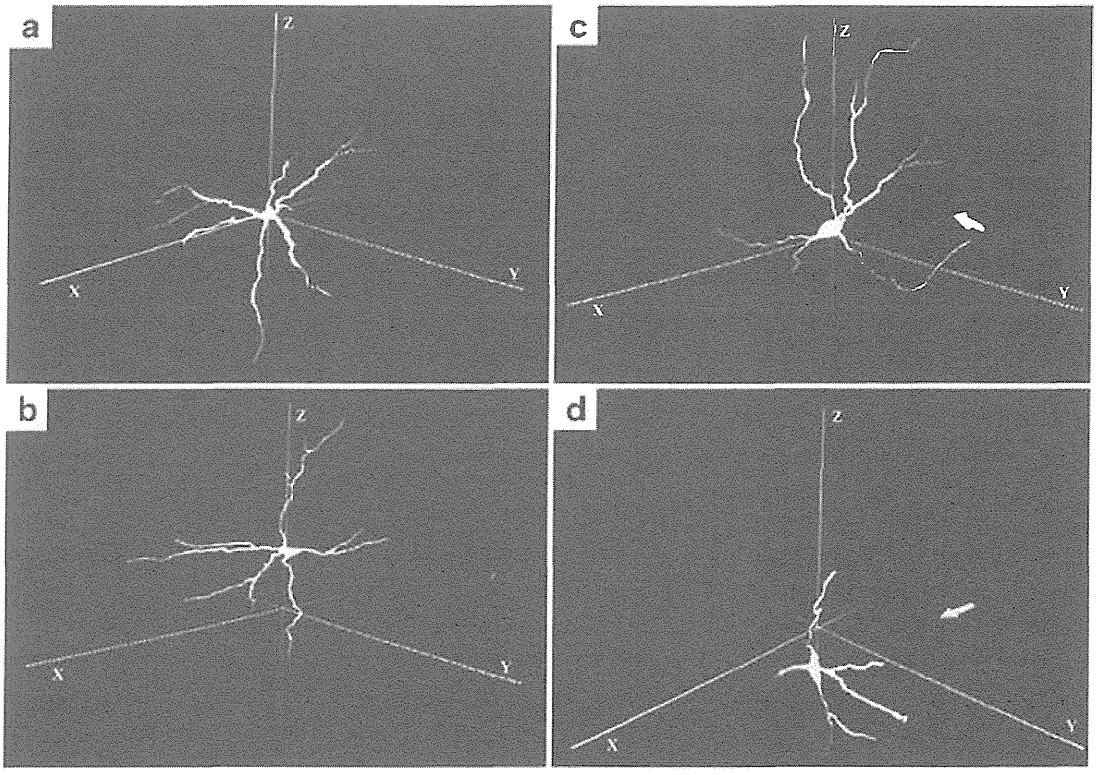

Fig. 9.2 Three-dimensional computer display of the dendritic arborization of the wheat germ agglutinin-horseradish peroxidase-labeled spinal accessory motoneurons (*abscissa* lateral direction, *ordinate* anteroposterior direction, and *z*-axis longitudinal direction). The compression force is applied in the *x*–*y* plane marked by *arrows* in (**c**) and (**d**). (**a**) Motoneuron at C2–C3 segment in the control ICR mouse; (**b**) site A in the *twy* mouse, the most rostral level; (**c**) site B, the level immediately rostral to the compressive lesion; (**d**) site C, the compression level at the C2–C3 cord segments (Reprinted, with permission, from [7])

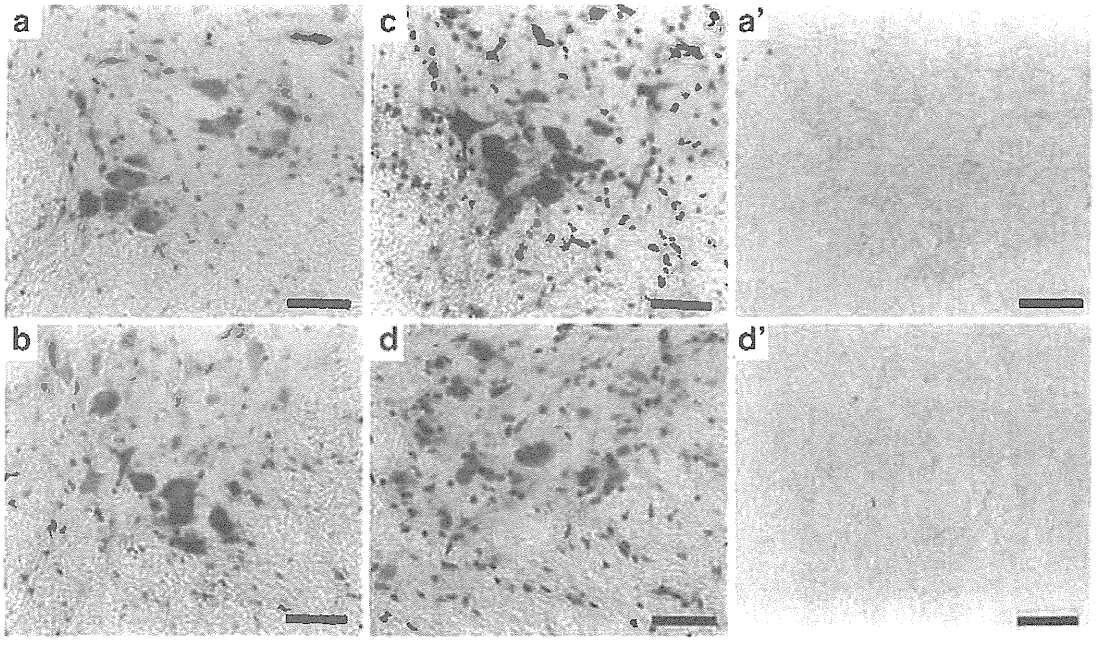

Fig. 9.3 Photomicrographs showing localization of immunoreactivity of brain-derived neurotropic factor in the anterior gray horn of a representative ICR mouse (**a**) and *twy* mouse (**b**–**d**) with a transverse remnant area of 60 %. (**b**) Site A; (**c**) site B; (**d**) site C. (**a′**, **d′**) Negative controls for ICR and *twy* mice, respectively. *Top* posterior aspect of the spinal cord. Scale bars = 50 μm (Reprinted, with permission, from [7])

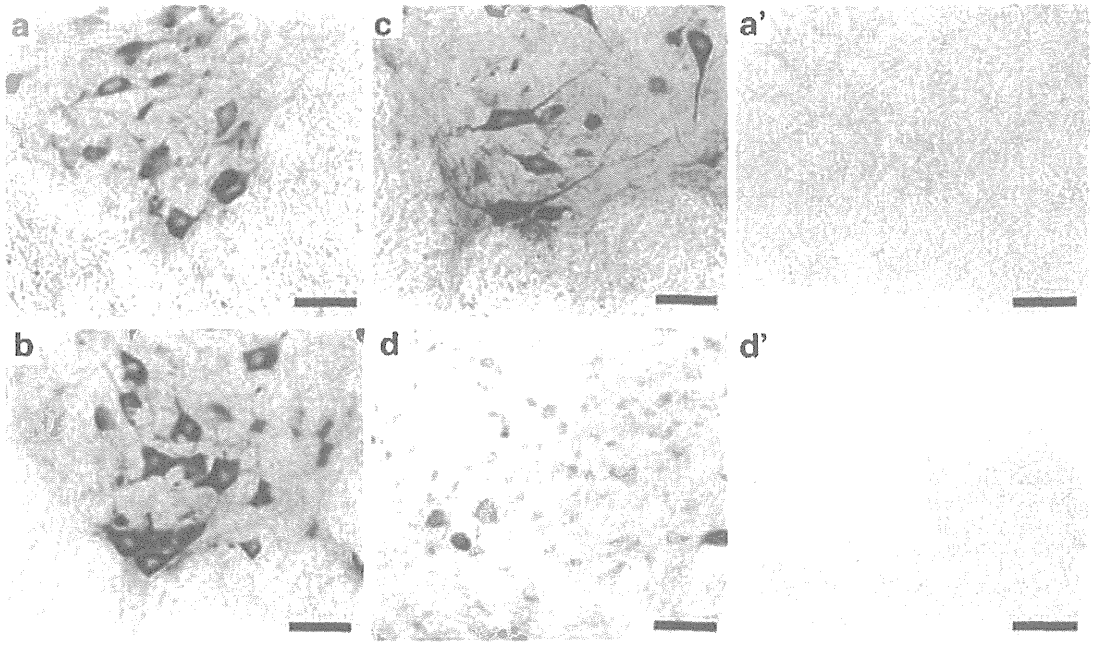

Fig. 9.4 Photomicrographs showing localization of immunoreactivity of neurotrophin-3 in a representative control ICR mouse (**a**) and *twy* mouse with a transverse remnant area of 55 % (**b–d**). (**b**) Site A; (**c**) site B; (**d**) site C. (**a′**, **d′**) Negative controls for ICR and *twy* mice, respectively. *Top*, dorsal aspect of the cord. Scale bars = 50 μm (Reprinted, with permission, from [7])

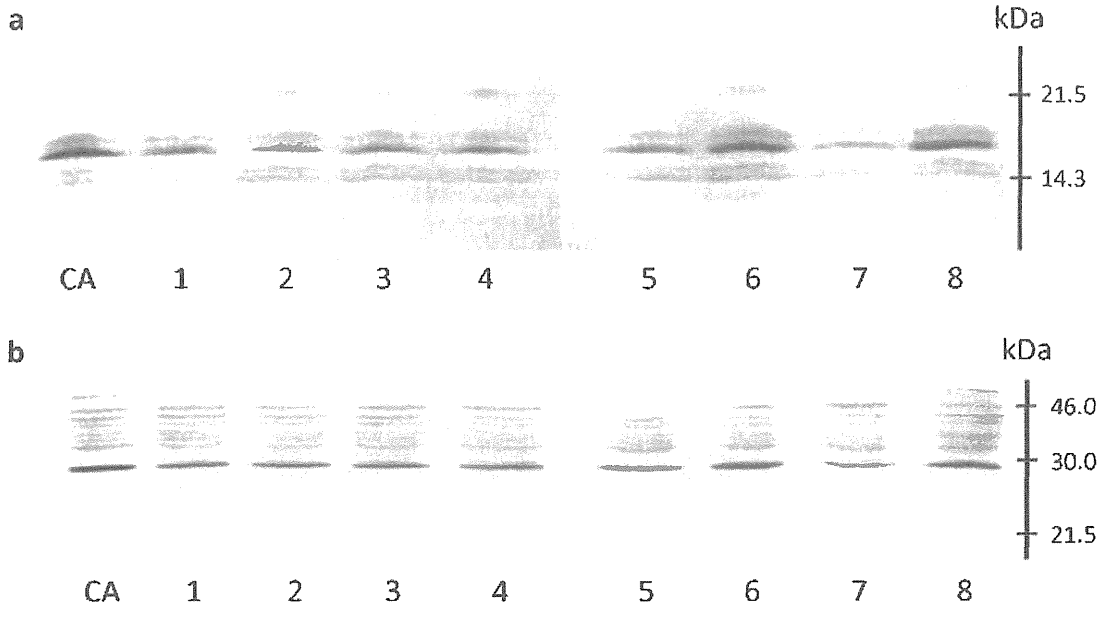

Fig. 9.5 Photomicrograph showing the expression of brain-derived neurotropic factor (**a**) and neurotrophin-3 (**b**) by Western blot analysis. The lane number shows each level of the spinal cord in the ICR (*lanes 1–4*) and *twy* (*lanes 5–8*) mice; *CA* refers to the hippocampus. *Lanes 1* and *5* in site A, the level most rostral to the C1 ventral root; *lanes 2* and *6* in site B, the level immediately rostral to compression between C1 ventral and C2 dorsal roots; *lanes 3* and *7* site C, between C2 and C3 dorsal roots (the compressed level in the *twy* mouse); *lanes 4* and *8*, the level between C3 and C4 dorsal roots (Reprinted, with permission, from [7])

9.1.6 *TUNEL Staining in the* twy/twy *Mouse Spinal Cord*

Figure 9.6 shows the topographic distribution of TUNEL-positive cells in the chronically compressed spinal cord of moderately and severely compressed *twy/twy* mouse examined by the TUNEL method. No TUNEL-positive cells were identified in both the gray and white matters of the control ICR mouse spinal cord. In contrast, TUNEL-positive cells were found in the gray and white matter in the *twy/twy* mouse with moderate compression. In comparison, fewer TUNEL-positive cells are found in the severe compression group particularly in the anterior horn, though these cells were abundant particularly in the anterior columns.

9.2 Discussion

Using the *twy* mice, we have previously demonstrated a significant reduction in the number of anterior horn cells at the level of mechanical compression [6, 7]. A progressively smaller number of these cells was noted when TRAS was 70 % of the normal value, reaching an asymptote approximately below 50 %. Interestingly, we also found increased population of spinal accessory motoneurons at levels rostral to the C1 vertebra (sites free of direct mechanical compression) [12]. The latter finding led us to speculate that a group of motoneurons may translocate rostrally to avoid chronic mechanical compression. Rostral to the site of mechanical compression (site B), we found enlargement of neuron soma and dendritic elongation of the WGA-HRP-labeled accessory motoneurons, which correlated significantly with deterioration of TRAS values measured at the site of compression. Somal size and dendritic arborization increase in order to facilitate synaptic connection [13] representing enhanced synaptic circuits [14, 15] to compensate the compromised function of spinal cord motoneurons.

Nerve growth factors, such as BDNF and NT-3, promote development of neurite outgrowth, growth, and differentiation of neurons, as well as their survival [16]. Our study found increased BDNF and NT-3 immunoreactivities in anterior horn cells, in close association with increased neuronal density of spinal accessory motoneurons when TRAS ranged between 50 % and 70 %. We postulate that considerable amounts of neuropeptides are transported retrogradely [17–19] and/or from the brain [20] in order to increase neuronal activity as well as axonal transport. It is known that astroglial cells produce BDNF [21] and other nerve growth factors [22]. In *twy* mice, when TRAS was 55 % of the control, a number of infiltrated astroglial cells, positive for BDNF immunostaining, were detected at sites rostral to the site of compression, related to increased number of motoneurons: another possible mechanism to enhance neuronal repair and regeneration. The present study demonstrated increased numbers of TUNEL-positive neurons in the gray matter and oligodendrocytes in the white matter of the spinal cord of the *twy/twy* mouse with progressive mechanical compression, which probably contributes to axonal degeneration and demyelination in the *twy/twy* mouse spinal cord with severe compression [8].

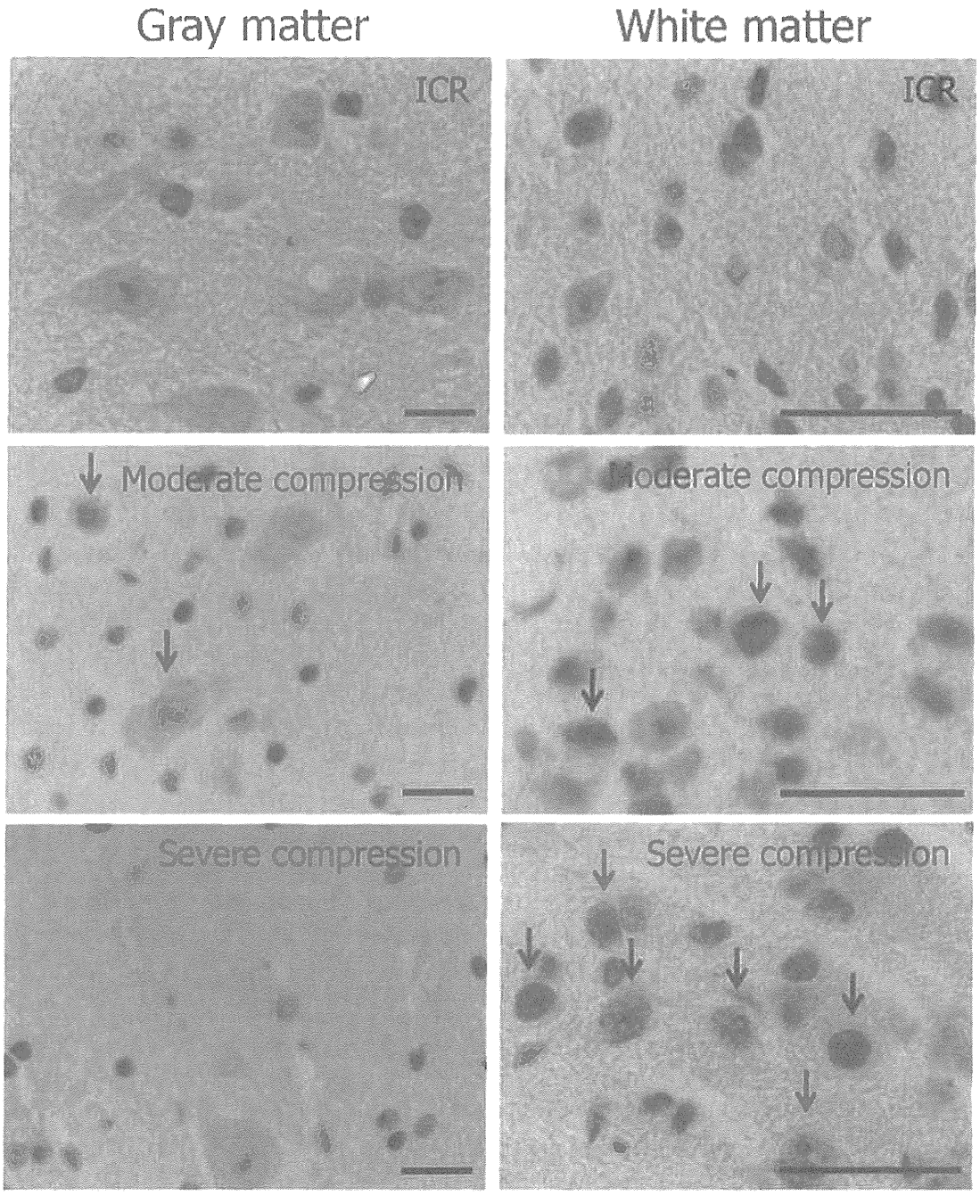

Fig. 9.6 Photomicrographs of terminal deoxynucleotidyl transferase (TdT)-mediated dUTP nick-end labeling (TUNEL) staining in representative control ICR mice (*upper photos*) and *twy/twy* mice with moderate compression (*middle photos*) or severe compression (*lower photos*). *Left column*: photomicrographs taken by a roupe (×3). The *white rectangular area* (anterior horn of the gray matter) and *black rectangular area* (anterior column of the white matter) are enlarged in the same row in the *middle* and *right columns*, respectively. *Black arrows*: representative TUNEL-positive cells. TUNEL-positive cells in the gray and white matter are noted in *twy/twy* mouse. Scale bars = 50 μm

9.3 Conclusion

WGA-HRP-labeled accessory motoneurons expressed significant BDNF and NT-3 immunoreactivities that correlated with enlargement of neuronal soma and extensive dendritic arborization at levels rostral to the site of mechanical compression. Astroglial cells at these levels may play a role in neuronal reserve and survival. There is a significant correlation between the proportion of apoptotic neurons and oligodendrocytes in the compressed area of the spinal cord and the magnitude of cord compression.

Acknowledgment This work was supported in part by Grants-in-Aid for General Scientific Research of the Ministry of Education, Science and Culture of Japan (grants numbers 09671480, C15591571, B16390435, B18390413, and B19791023). This work was also supported in part by grants from the Investigation Committee on Ossification of the Spinal Ligaments, Public Health Bureau of the Japanese Ministry of Health and Welfare.

Conflict of Interest All authors declare that they have no conflict of interest.

References

1. Baba H, Uchida K, Maezawa Y et al (1996) Lordotic alignment and posterior migration of the spinal cord following en bloc open-door laminoplasty for cervical myelopathy: a magnetic resonance imaging study. J Neurol 243:626–632
2. Baba H, Maezawa Y, Uchida K et al (1997) Plasticity of the spinal cord contributes to neurological improvement after treatment by cervical decompression. A magnetic resonance imaging study. J Neurol 244:455–460
3. Mizuno J, Nakagawa H, Iwata K et al (1992) Pathology of spinal cord lesions caused by ossification of the posterior longitudinal ligament, with special reference to reversibility of the spinal cord lesion. Neurol Res 14:312–314
4. al-Mefty O, Harkey HL, Marawi I et al (1993) Experimental chronic compressive cervical myelopathy. J Neurosurg 79:550–561
5. Martin D, Schoenen J, Delree P et al (1992) Experimental acute traumatic injury of the adult rat spinal cord by a subdural inflatable balloon: methodology, behavioral analysis, and histopathology. J Neurosci Res 32:539–550
6. Baba H, Maezawa Y, Imura S et al (1996) Quantitative analysis of the spinal cord motoneuron under chronic compression: an experimental observation in the mouse. J Neurol 243:109–116
7. Uchida K, Baba H, Maezawa Y et al (1998) Histological investigation of spinal cord lesions in the spinal hyperostotic mouse (*twy/twy*): morphological changes in anterior horn cells and immunoreactivity to neurotropic factors. J Neurol 245:781–93
8. Inukai T, Uchida K, Nakajima H et al (2009) Tumor necrosis factor-alpha and its receptors contribute to apoptosis of oligodendrocytes in the spinal cord of spinal hyperostotic mouse (*twy/twy*) sustaining chronic mechanical compression. Spine 34:2848–57
9. Henderson CE, Camu W, Mettling C et al (1993) Neurotrophins promote motor neuron survival and are present in embryonic limb bud. Nature 363:266–270
10. Sendtner M, Holtmann B, Kolbeck R et al (1992) Brain-derived neurotrophic factor prevents the death of motoneurons in newborn rats after nerve section. Nature 360:757–759

11. Yan Q, Elliott JL, Matheson C et al (1993) Influences of neurotrophins on mammalian motoneurons in vivo. J Neurobiol 24:1555–1577
12. Baba H, Maezawa Y, Uchida K et al (1997) Three-dimensional topographic analysis of spinal accessory motoneurons under chronic mechanical compression: an experimental study in the mouse. J Neurol 244:222–229
13. Koziol JA, Tuckwell HC (1978) Analysis and estimation of synaptic densities and their spatial variation on the motoneuron surface. Brain Res 150:617–624
14. Purves D, Lichtman JW (1985) Geometrical differences among homologous neurons in mammals. Science 228:298–302
15. Turner AM, Greenough WT (1985) Differential rearing effects on rat visual cortex synapses. Synaptic and neuronal density and synapses per neuron. Brain Res 329:195–203
16. Funakoshi H, Frisen J, Barbany G et al (1993) Differential expression of mRNAs for neurotrophins and their receptors after axotomy of the sciatic nerve. J Cell Biol 123:455–465
17. DiStefano PS, Friedman B, Radziejewski C et al (1992) The neurotrophins BDNF, NT-3, and NGF display distinct patterns of retrograde axonal transport in peripheral and central neurons. Neuron 8:983–993
18. Maisonpierre PC, Belluscio L, Friedman B et al (1990) NT-3, BDNF, and NGF in the developing rat nervous system: parallel as well as reciprocal patterns of expression. Neuron 5:501–509
19. Zhou XF, Rush RA (1993) Localization of neurotrophin-3-like immunoreactivity in peripheral tissues of the rat. Brain Res 621:189–199
20. Ernfors P, Persson H (1991) Developmentally regulated expression of HDNF/NT-3 mRNA in rat spinal cord motoneurons and expression of BDNF mRNA in embryonic dorsal root ganglion. Eur J Neurosci 3:953–961
21. Barde YA, Edgar D, Thoenen H (1982) Purification of a new neurotrophic factor from mammalian brain. EMBO J 1:549–553
22. Lu B, Yokoyama M, Dreyfus CF et al (1991) NGF gene expression in actively growing brain glia. J Neurosci 11:318–326

ELSEVIER

CrossMark

The Spine Journal 14 (2014) 1601–1610

THE SPINE JOURNAL

Clinical Study

Prognostic value of changes in spinal cord signal intensity on magnetic resonance imaging in patients with cervical compressive myelopathy

Kenzo Uchida, MD, PhD, Hideaki Nakajima, MD, PhD*, Naoto Takeura, MD, Takafumi Yayama, MD, PhD, Alexander Rodriguez Guerrero, MD, Ai Yoshida, MD, Takumi Sakamoto, MD, Kazuya Honjoh, MD, Hisatoshi Baba, MD, PhD

Department of Orthopaedics and Rehabilitation Medicine, Faculty of Medical Sciences, University of Fukui, 23-3 Matsuokashimoaizuki, Eiheiji-cho, Yoshida-gun, Fukui 910-1193, Japan

Received 22 September 2012; revised 3 September 2013; accepted 19 September 2013

Abstract

BACKGROUND CONTEXT: Signal intensity on preoperative cervical magnetic resonance imaging (MRI) of the spinal cord has been shown to be a potential predictor of outcome of surgery for cervical compressive myelopathy. However, the prognostic value of such signal remains controversial. One reason for the controversy is the lack of proper quantitative methods to assess MRI signal intensity.

PURPOSE: To quantify signal intensity and to correlate intramedullary signal changes on MRI T1- and T2-weighted images (WIs) with clinical outcome and prognosis.

STUDY DESIGN: Retrospective case study.

PATIENT SAMPLE: Patients (n=148; cervical spondylotic myelopathy, n=102 and ossified posterior longitudinal ligament, n=46) who underwent surgery for cervical compressive myelopathy and had high signal intensity change on sagittal T2-WI MRI before surgery between 2006 and 2010.

OUTCOME MEASURE: Neurologic assessment was conducted with the Japanese Orthopedic Association (JOA) scoring system for cervical myelopathy. The rate of neurologic improvement was calculated with the use of preoperative and postoperative JOA scores.

METHODS: Quantitative analysis of MRI signal on both T1- and T2-WIs via use of the signal intensity ratio (SIR; signal intensity of lesion relative to that at C7-T1 disc level) was performed. Correlations between SIR on T1- and T2-WIs and preoperative JOA score, JOA improvement rate, disease duration, and MRI morphologic classification (cystic or diffuse type) were analyzed. Multivariate regression analysis for JOA improvement rate was also analyzed. In a substudy, 25 patients underwent follow-up MRI starting from 6 months after surgery to analyze the relationship between changes in SIR on follow-up MRI and clinical outcome.

RESULTS: SIR on T1-WIs, but not SIR on T2-WIs, correlated with postoperative neurologic improvement. The disease duration correlated negatively with SIR on T1-WIs and JOA improvement rate but not with SIR on T2-WIs. SIR on T2-WIs of "cystic type" was significantly greater than of "diffuse type," but SIR on T1-WI and JOA improvement rate were not different in the two types. Stepwise multivariate regression analysis indicated that SIR on T1-WIs and long disease duration were significant predictors of postoperative neurologic outcome. SIR on follow-up T1-WI and changes in SIR on T1-WI after surgery correlated positively with postoperative improvement rate. SIR on follow-up T2-WI and changes on T2-WI correlated negatively with postoperative neurologic improvement.

CONCLUSIONS: Our results suggest that low intensity signal on preoperative T1-WIs but not T2-WIs correlated with poor postoperative neurologic outcome. Furthermore, decreased signal

FDA device/drug status: Not applicable.

Author disclosures: ***KU:*** Nothing to disclose. ***HN:*** Nothing to disclose. ***NT:*** Nothing to disclose. ***TY:*** Nothing to disclose. ***ARG:*** Nothing to disclose. ***AY:*** Nothing to disclose. ***TS:*** Nothing to disclose. ***KH:*** Nothing to disclose. ***HB:*** Nothing to disclose.

Disclaimer: None of the authors has any financial ties to any commercial party.

* Corresponding author. Department of Orthopaedics and Rehabilitation Medicine, Faculty of Medical Sciences, University of Fukui, 23-3 Matsuokashimoaizuki, Eiheiji-cho, Yoshida-gun, Fukui 910-1193, Japan. Tel.: (81) 776-61-8383l; fax: (81) 776-61-8125.

E-mail address: nhideaki@u-fukui.ac.jp (H. Nakajima)

1529-9430/$ - see front matter © 2014 Elsevier Inc. All rights reserved.
http://dx.doi.org/10.1016/j.spinee.2013.09.038

intensity on postoperative T1-WIs and increased signal intensity on postoperative T2-WIs are predictors of poor neurologic outcome. © 2014 Elsevier Inc. All rights reserved.

Keywords: Cervical myelopathy; Magnetic resonance imaging; Intramedullary spinal cord signal intensity; Quantitative analysis; Prognosis; Neurologic outcome

Introduction

It is important to assess spinal cord function in patients with cervical compressive myelopathy that is amenable to neurosurgical treatment. Most conventional tests focus on evaluation of neural conductivity across the damaged spinal cord [1] or morphologic and pathologic changes at the compressed cord that can be identified on magnetic resonance imaging (MRI). MRI is a valuable tool before surgical decompression because it visualizes not only the magnitude of spinal cord compression but also intramedullary signal intensity. Many authors have reported intramedullary changes in high signal intensity on T2-weighted imaging (WI) in patients with compressive spondylotic lesions of the cervical spinal cord [2–5]. The presence of intramedullary high signal intensity on T2-WI in patients with compressive myelopathy reflects chronic spinal cord compression lesion. However, the prognostic value of these imaging abnormalities remains controversial, especially with regard to signal intensity of the spinal cord on T2-WI. Intramedullary changes in high signal intensity on T2-WI can reflect a wide range of compressive pathologies and nonspecific histologic changes that have been related to different events, representing anything from mild, reversible changes such as gliosis and demyelination to severe, irreversible changes including cavitation or necrosis. A few studies have shown a clear correlation between high signal intensity of the spinal cord on T2-WI alone and poor prognosis after surgery and that poor prognosis correlates with low signal intensity of the spinal cord on T1-WI [6,7]. Other studies also showed that high signal intensity on T2-WI of the spinal cord and low T1-weighted signal intensity of the spinal cord can predict a poor surgical outcome. However, controversy exists in the reported results, mainly because of the lack of proper quantitative assessment method of these changes in signal intensity. The present study was designed to quantify signal intensity and to correlate changes in intramedullary signal on MRI with clinical outcome and determine their prognostic value.

Materials and methods

Patient population

Between 2006 and 2010, a total of 148 patients (CSM, n=102; OPLL, n=46) who underwent decompressive surgery at our hospital and showed high intramedullary signal intensity of the spinal cord on sagittal T2-weighted magnetic resonance imaging (MRI; 1.5 Tesla Signa System; General Electric, Milwaukee, WI) were assessed in this study. None of the patients had developmentally narrow canal on plain radiographs or multisegmental lesions on MRI. Exclusion criteria included a history of traumatic injury of the cervical spinal cord, malignancy, and infection. Among the 148 patients, 25 underwent follow-up MRI starting from 6 months after operation. Two senior surgeons (KU, HB) performed all operations, and they did not participate in the assessment of MRIs and statistical analysis. All examinations strictly followed the Ethics Review Committee Guidelines of Fukui University, and written informed consent was obtained from all patients.

Neurologic assessment was conducted by use of the Japanese Orthopedic Association (JOA) scoring system for cervical myelopathy (Table 1). The rate of neurologic improvement was calculated by the use of the following equation: [(postoperative JOA score−preoperative JOA score)/(17−preoperative JOA score)×100]. An improvement rate of 100% was the best possible postoperative recovery [8].

High-resolution MRI

MRI examination of the spinal cord was performed preoperatively using 1.5 Tesla Signa System (General Electric). T1-WIs and T2-WIs of sagittal views of the spinal cord were obtained using spin echo sequence system for T1-WIs and a fast spin echo sequence system for T2-WIs. Quantitative analysis was based on the method described previously [9]. T2-WIs of sagittal increased signal intensity values on the cervical spinal cord were obtained first because small changes in signal intensity on T1-WIs are difficult to visualize, and 0.05 cm^2 regions of interest (ROIs) were taken. The same spinal cord lesion of T1-WIs on T2-WIs were obtained on Centricity Picture Archiving and Communication Systems (General Electric Healthcare Japan, Tokyo, Japan), and 0.05cm^2 ROIs were taken. The signal intensity values for T2- and T1-WIs of sagittal views of the normal cord at cervical C7-T1 disc levels were obtained, and 0.3 cm^2 ROIs were selected. The signal intensity was measured automatically by the computer, and changes in signal intensity in the cord were qualitatively assessed on both T1-WIs and T2-WIs. For quantitative analysis of the signal, the signal intensity ratio (SIR) for both T1-WIs and T2-WIs was calculated by the following equation:

$$\mathrm{SIR} = \left[\text{SI of sagittal cervical and spinal cord lesion } \left(0.05\ \mathrm{cm}^2\right) / \text{SI of sagittal normal cord between C7 and T1 disc levels } \left(0.3\ \mathrm{cm}^2\right)\right]$$